Structural Integrity Assessment of Thick Wall Pipes under Biaxial Loading

D. Arafah[1*], M. Madia[1], S. Beretta[1] and M. Cristea[2]

[1] Politecnico di Milano, Department of Mechanical Engineering, Via La Masa 1, I-20156 Milano, Italy

[2] TENARIS Dalmine, R&D, Piazza Caduti 6 Luglio 1944, I-24044 Dalmine, Italy

[*] diya.arafah@mail.polimi.it

Keywords: pipes, burst test, biaxial loading, FEM, SINTAP/FITNET.

Abstract. The present work deals with the numerical and analytical assessment of the burst pressure for capped ends thick pipes containing artificial axial narrow defect onto the outer surface. The effect of the capped ends on the burst pressure is well known as the biaxial stress state. In order to estimate the effect of biaxial loading, the European procedure SINTAP/FITNET based on simple models available in literature is applied.
In the present paper, a methodology based on finite element analysis simulations which allows to improve the result accuracy and catch the real behaviour of the burst tests observed experimentally is presented. The predicted burst pressure has been found to be 6% higher than the one obtained on models with free ends, due to biaxial loading.
Substantial improvement of the burst pressure prediction is obtained when the full state of stress is considered in the analytical procedure.

1. Introduction

The structural assessment of pressurized components is an important issue in many engineering applications, such as the nuclear and oil & gas industries, in which the risk of failure for these components must be minimized due to the severe failure consequences [1]. In case of steel components, the presence of defects given by technological and production processes must be taken into account, as the propagation of these small defects due to fatigue can lead to the formation of cracks and, in the worst case, to the unexpected fracture of the component [2]. It is therefore important to perform experimental tests in order to assess the load-carrying capacity of the component containing cracks of different sizes and shapes. In particular, in case of pressurized components, very often burst tests are carried out in order to evaluate the maximum pressure which the cracked component can withstand. The burst test for pipes is usually carried out onto a piece of pipe in which both ends are capped by a circumferential welding in order to undergo a high internal pressure [3].
In order to predict the limit burst pressure for the present application, an analytical calculation guideline is needed.
When a structural integrity assessment is performed using R6 [4], the limit load of a defective structure must be defined. The limit load may be defined according to the plastic deformation behavior of either the overall defective structure (global limit load) or that in the crack ligament (local limit load). A global limit load is the load at which the load–point displacement becomes unbounded and is relevant to the failure of the whole structure. A local limit load corresponds to a loading level at which gross plasticity occurs in the crack ligament and may be relevant to ligament failure. The local limit load is always less than or equal to the global limit load for a cracked structure and, therefore, yields conservative results in an assessment.

A limit load review by Miller [5] contains solutions for cylinders with through-wall, surface and extended surface axial defects under internal pressure. Further solutions for cylinders with axial defects were developed by Carter [6]. Staat [7,8] modified some of Carter's solutions for thin-walled cylinders to extend them to thick-walled cylinders and compared the modified solutions with experimental data. Recently, Staat et al. [9] improved the solutions further by considering the influence of the opposite unflawed section of the wall. Lei [10] summarized the limit load solutions for cylinders with axial cracks, and developed new local and global solutions.

In this paper the assessment of burst pressure for capped end pipe specimens, containing at mid-length an external axial flaw, has been performed by both numerical (FEM) and analytical methods. In capped end burst tests, as the pipe is stretched in the longitudinal direction, the effect of the biaxial loading has been taken into account. Moreover, the radial stress cannot be neglected in case of thick wall pipes with high internal pressures. Therefore, analytical approaches have been identified to properly estimate burst pressure under actual testing conditions.

2. Material and experimental tests

2.1 Material Properties. The material under investigation is a high strength - high toughness steel grade. The material properties at test temperature (-20° C) are: Young's modulus E = 211000 MPa and yield strength $R_{p0.2}$ = 655 MPa. The true stress-strain curve is shown in Fig. 1.

2.2 Experimental tests. The burst tests have been conducted by TENARIS Dalmine on thick-walled pipes with capped ends at -20° C. Fig. 2 shows the schematic of the flawed pipe, the cracks have been assumed to have a semi-elliptical shape described by a length 2*c* and a maximum depth *a*. The dimensions of the pipe and the defect under investigation are provided in Table 1, the selected geometry is classified as thick wall pipe.

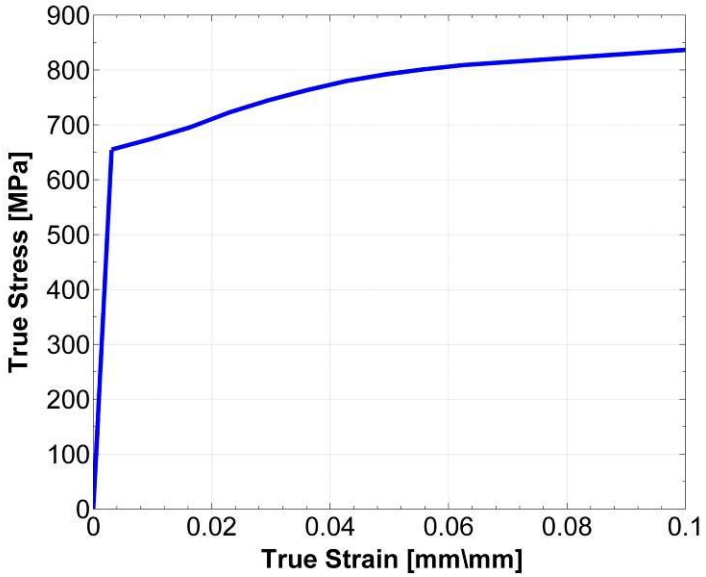

Fig. 1. Monotonic true stress-strain curve at -20°C.

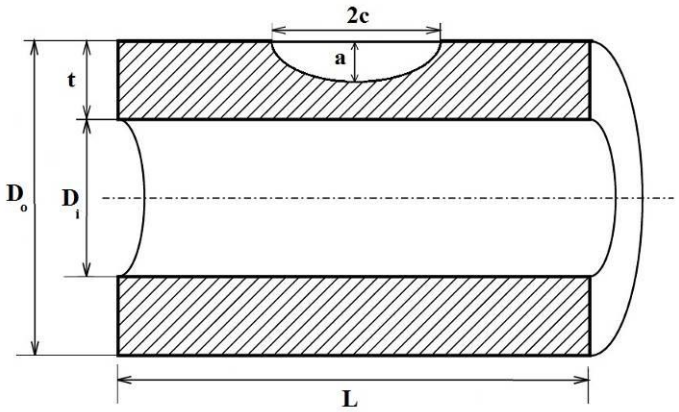

Fig. 2. Schematic of the pipe with external surface axial crack.

Fig. 3a shows the state of the pipe at the end of the test, in all cases the pipes fail because of burst and they do not show leak before break (LBB). Furthermore, for each pipe a fractographic analysis has been carried out in order to understand the origin and the cause of the failure (see Fig. 3b): after an initial stage of ductile tearing, the crack grows unstable starting from a point which is beneath the surface.

Table 1. Pipe and defect size.

Pipe dimensions [11]		
Outer Diameter D_o [mm]	Inner Diameter D_i [mm]	Pipe Length L [mm]
155	125	400
Defect		
Specimen	Defect Depth a [mm]	Defect Length $2c$ [mm]
5	5.8	15

a)  b) 

Fig 3. Burst test of the specimen #5: a) longitudinal fracture at the end of the test; b) fractography of the broken piece.

3. Numerical model

3.1 Model generation. Three dimensional finite element analyses for both free ends and capped ends pipes have been performed using the finite element code ABAQUS 6.9 [12].

Preliminary analysis on the uncracked pipe have been carried out; due to the symmetry only one-eighth of the pipe has been considered (see Fig. 4).

Calculations of the stress intensity factor (SIF) and *J*-integral in the elastic-plastic domain of the cracked pipes have been performed using the submodeling technique due to the high mesh refinement required along the crack front [13, 14]. The results from the global model are

interpolated on the submodel boundary and used to drive the submodel. Fig. 5 shows the mesh used for the global model and the submodel, in both cases hexahedral quadratic elements have been employed (C3D20 [12]).

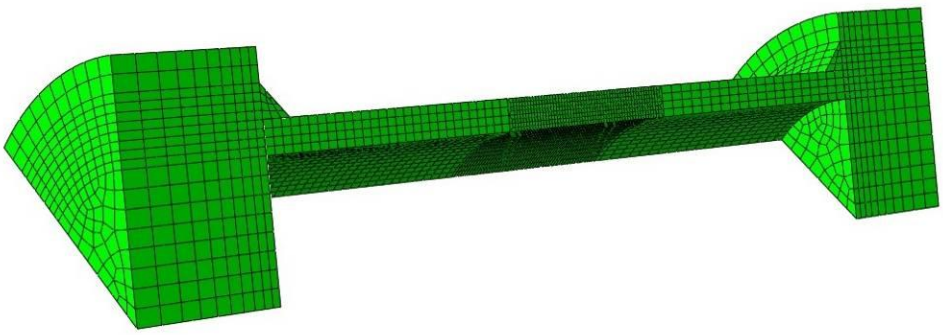

Fig 4. Model of the uncracked pipe with capped ends.

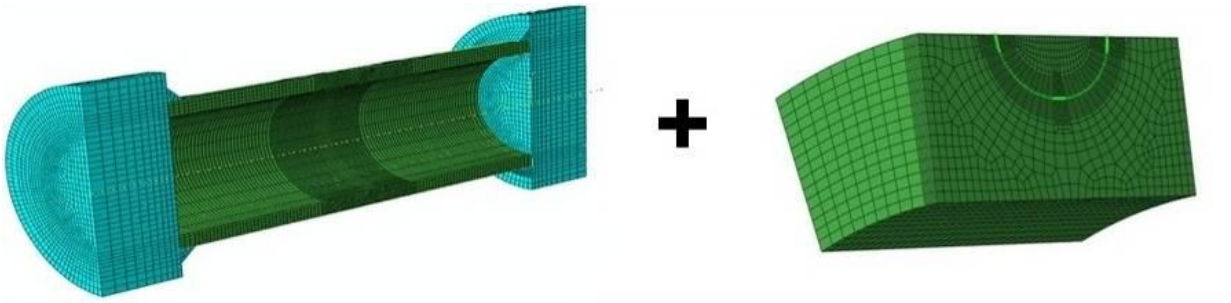

Fig 5. Global model and submodel with highly refined mesh in the case of pipe with capped ends.

3.2 Mesh verification. The model of the uncracked pipe has been used to verify the quality of the mesh for a correct representation of the stress field through the wall of the pipe and to check the edge effects for the pipe with capped ends. In particular Fig. 6a shows the comparison between the stresses obtained for the pipe with capped and free ends. In addition, it must be remarked that the stresses derived from the numerical simulations have been verified to be in good agreement with the analytical stresses for thick-walled pipes [15]. Furthermore, the total length of the pipe sample has been found to be large enough to prevent the influence of edge effects on the stress field at the mid-section of the pipe (see Fig. 6b), where the artificial notches have been machined.
To the aim of verifying the mesh quality for the fracture mechanics analysis, the SIF values obtained by submodeling at the surface (B) and deepest (A) point of the crack have been compared with the analytical solution provided by Newman-Raju [16] as shown in Fig. 6c, the numerical results provided reliable estimates for a wide pressure range (difference lower than 5%).

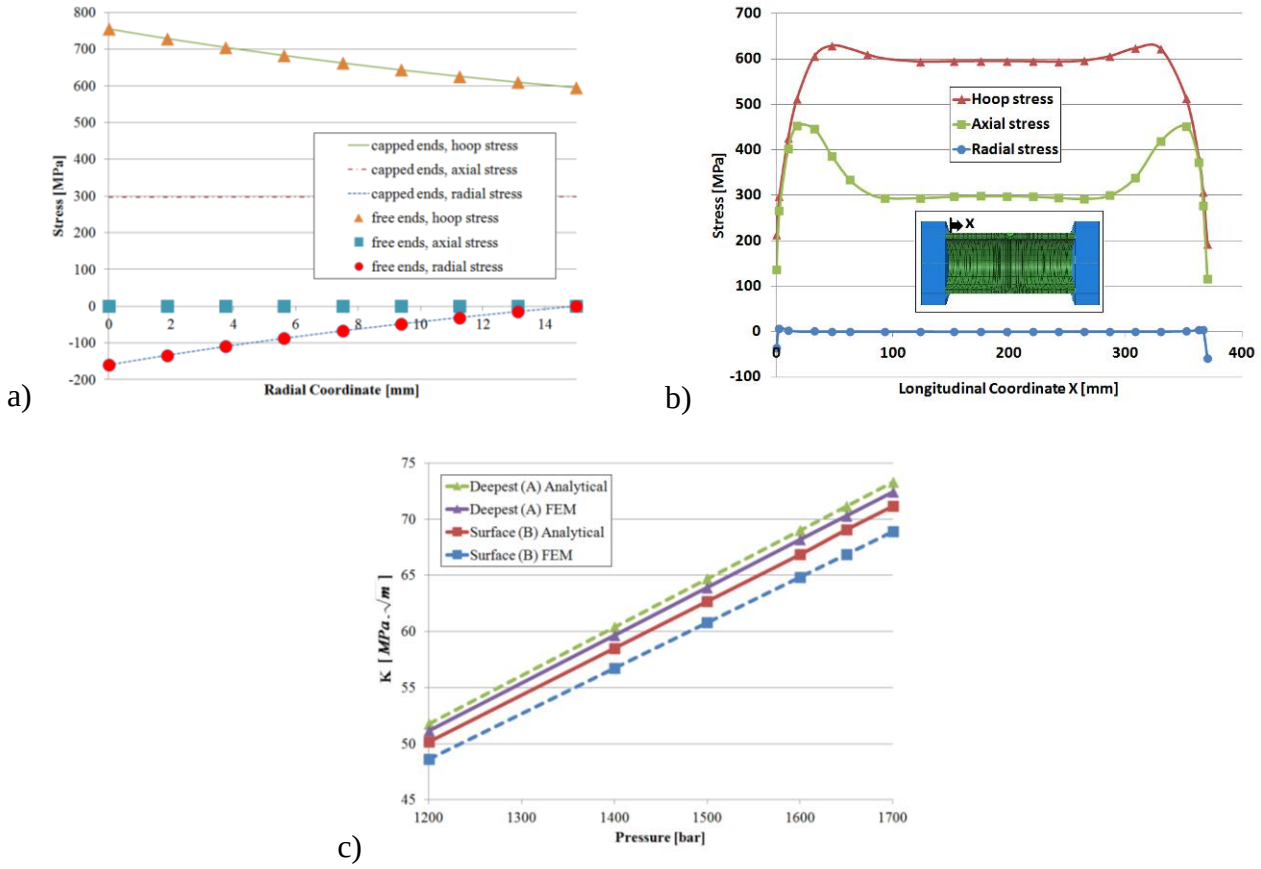

Fig 6. Analyses for mesh verification: a) stress comparison between simulations on pipe with free and capped ends; b) influence of the edge effects; c) comparison of the numerically derived stress intensity factors with the analytical solutions [16].

4. Results and Discussion

4.1 Numerical Solution. In order to assess the burst pressure of the pipe with an artificial axial defect, elastic-plastic finite element analyses have been carried out. The first step consisted in the analysis of the *J*-integral values along the crack front for increasing pressure values. Fig. 7 shows that the maximum value of the *J*-integral occurs in a sub-surface point at a distance of about 3.2 mm along the crack front coordinate ξ (about 30° from the outer surface), which is also in agreement with the outcomes of the fractography (see Fig. 3b) that shows an initial fracture at the same coordinate position. Already an important conclusion can be drawn: the structural assessment based on the surface point B and the deepest point A (as suggested by the current structural integrity guidelines [4,17]) would lead to the misleading conclusion that the pipe would fail in a LBB mode due to the larger *J*-integral values at the deepest point, compared with the ones at the surface point. Due to the variation of the triaxiality of stress state along the crack front [18,19], the maximum *J*-integral is located under the surface, the sub-surface point C must be used in the failure assessment of the pipe, thus giving the correct conclusion that the pipe bursts.

Fig. 8 shows the different estimated burst pressure for a pipe with free and capped ends. The burst pressure for the model with free ends is approximately 100 bar lower than the burst pressure obtained from the simulations on the pipe with capped ends. Anyhow, the estimated burst pressures remain lower than the experimentally derived value, which is about 1650 bar. The difference between having the caps or not is due to the fact that the pipe with capped ends is stretched in the

longitudinal direction, which turns in a reduction of the crack opening displacement, hence a reduction of the crack driving force.

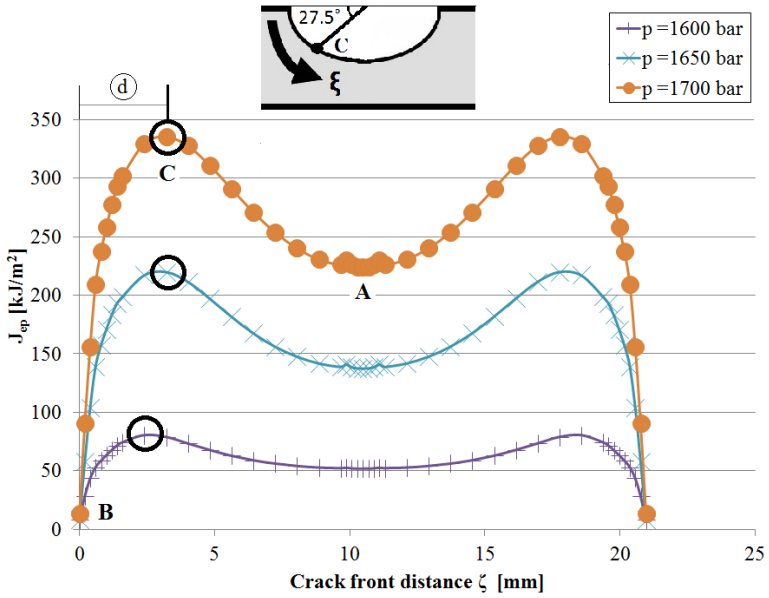

Fig. 7. *J*-integral along the crack front for the simulation with capped ends.

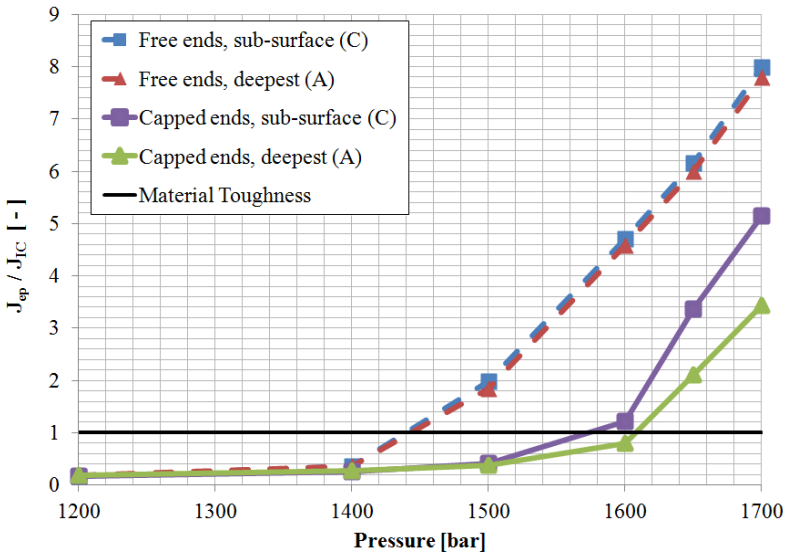

Fig. 8. *J*-integral as function of the applied internal pressure.

4.2 Analytical model

The SINTAP/FITNET procedure has been applied to predict the burst pressure, in particular the structural integrity assessment has been carried out referring to a crack driving force approach (CDF) [17]. The advantage of CDF approach is the separation between the material and the loading side. The CDF procedure is given by the following equation:

$$J_{ep} = J_e \times \left[f\left(L_r\right) \right]^{-2} \tag{1}$$

where $J_e = K^2/E$ is the elastic J-integral, $f(L_r)$ is the plastic correction function, and L_r is the ligament yielding parameter which is a measure of plasticity effects and is defined as the ratio of the loading condition being assessed to that required to cause plastic yielding of the structure. The analysis level 3 requires toughness data and the complete true stress-strain curve of the material to estimate J_{ep}. Then, referring to the definition of $f(L_r)$ in the analysis level 3, Eq. (1) can be rewritten as:

$$J_{ep} = J_e\left[\frac{E\varepsilon_{ref}}{\sigma_{ref}} + \frac{1}{2}L_r^2\frac{\sigma_{ref}}{E\varepsilon_{ref}}\right] \tag{2}$$

where σ_{ref} denotes the reference stress ($\sigma_{ref} = L_r \cdot \sigma_y$), and ε_{ref} is the reference strain at $\sigma = \sigma_{ref}$ determined from the true stress-strain curve.

The general plate model [20] has been used to evaluate the ligament yielding parameter L_r for the case of the pipe with free ends, whereas in the case of capped ends the effect of biaxial loading has been taken into account with simple models available in literature [21]:

$$L_{r,biaxial} = L_r.\sqrt{1-\lambda+\lambda^2} \tag{3}$$

$$\lambda = \frac{\sigma_{axial}}{\sigma_{hoop}} \tag{4}$$

The analytical J_{ep} estimates are compared with the finite element predictions in Fig. 9, in both cases, pipe with free and capped ends, the analytical values (dashed lines in Fig. 9) provide a non-conservative estimation of the burst pressure.

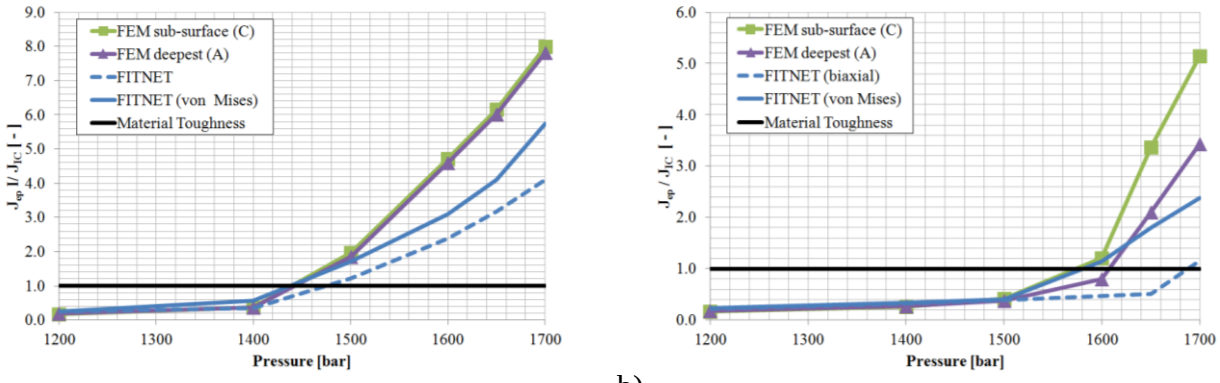

a) b)

Fig. 9. Analytical estimation of the burst pressure: a) pipe with free ends; b) pipe with capped ends.

The main issue which has been found to be the possible cause of this discrepancy is that thick-walled pipes experience a triaxial state of stress, given the high values of the radial stresses caused by the relevant amount of internal pressure. Therefore, to effectively predict the actual burst pressure, von Mises equivalent stress has been used in the analytical analysis to define the ligament yielding parameter:

$$L_r = \frac{\sigma_{vM}}{\sigma_y} \tag{5}$$

The new predictions speak in favor of a substantial improvement of the analytical procedure (see Fig. 9), if the full state of stress is considered, the analytical predictions match the results provided by the finite element analyses.

Conclusions

The present work deals with the numerical and analytical assessment of the burst pressure of axially cracked thick-walled pipes.

The analytical structural integrity assessment showed that the use of the hoop stress alone may provide non-conservative results, which is to say a predicted pressure higher than the experimental one. The main reason for this behavior is that thick-walled pipes undergo a triaxial state of stress since the radial stress cannot be neglected due to the high values of the internal pressure.

A substantial improvement of the analytical method for predicting the burst pressure is obtained when the full state of stress is considered through the von Mises equivalent stress.

Moreover, the elastic-plastic numerical analyses showed that the maximum *J*-integral is located under the surface due to the variation of the triaxiality of stress state along the crack front, thus giving the correct conclusion that the failure mode of the pipe is burst and not LBB. A pipe with capped ends has been found to have a burst pressure about 6% higher than the one for the pipe with free ends, because of the reduction of crack driving force induced by the longitudinal force.

Acknowledgement

Dr. Mario Rossi, director of Tenaris Dalmine Research & Development Center, is kindly acknowledged for permission to publish this work.

References

[1] G.A. Papadakis: Journal of Loss Prevention in the Process Industries 1999; 12:91-107.

[2] R. Doglione and D. Firrao: Int J Fatigue 1998; 20(2):161-168.

[3] J.B. Choi, B.K. Goo, J.C. Kim, Y.J. Kim and W.S. Kim: Int J Pres Ves Pip 2003; 80:121-128.

[4] R6: Assessment of the Integrity of Structures Containing Defects, Revision 4, British Energy Generation Ltd., 2001, with amendments to May 2007.

[5] AG. Miller: Review of limit loads of structures containing defects. Int J Pres Ves Pip 1988; 32:197-327.

[6] AJ. Carter: A library of limit loads for FRACTURE.TWO. Nuclear Electric Report TD/SID/REP/0191. Berkeley; 1991.

[7] M. Staat: Plastic collapse analysis of longitudinally flawed pipes and vessels. Nuclear Engineering and Design 2004; 234:25-43.

[8] M. Staat: Local and global collapse pressure of longitudinally flawed pipes and cylindrical vessels. Int J Pres Ves Pip 2005; 82:217-225.

[9] M. Staat, Vu Duc Khoi: Limit analysis of flaws in pressurized pipes and cylindrical vessels. Part I: axial defects. Eng Fract Mech 2007; 74:431-450.

[10] Y. Lei: A review of limit load solutions for cylinders with axial cracks and development of new solutions. Int J Pres Ves Pip 2008; 85:825-850.
[11] Tenaris Dalmine Spa, www.tenaris.com/italy
[12] Abaqus v6.9, Dassault Systemes.
[13] A. Diamantoudis and G. Labeas: Stress Intensity Factors of Semi-Elliptical Surface Cracks in Pressure Vessels by Global-Local Finite Element Methodology. Eng Fract Mech 2005; 72: 1299-1312.
[14] E. Marenic, I. Skozrit and Z. Tonkovic: On the calculation of stress intensity factors and J-integrals using the submodeling technique. J Pres Ves Tech 2010; 132(4).
[15] RG. Budynas: Advanced strength and applied stress analysis, 2nd ed., McGraw-Hill, New York, 1999.
[16] I. Raju and J. Newman: Stress-intensity factors for internal and external surface cracks in cylindrical vessels. J Pres Ves Tech 1982; 104:293-298.
[17] U. Zerbst, M. Schödel, S. Webster and R.A. Ainsworth: Fitness for service fracture assessment of structures containing cracks. Academic Press, 2007.
[18] W. Brocks, G. Künecke and K. Wobst: Stable crack growth of axial surface flaws in pressure vessels. Int J Pres Ves Pip 1989; 40:77-90.
[19] W. Brocks and G. Künecke: Elastic-plastic fracture mechanics analysis of a pressure vessel with an axial outer surface flaw. Nuclear Engineering and Design 1990; 119:307-315.
[20] S. Al Laham: Stress Intensity factor and limit load handbook. British Energy Ltd, 1998.
[21] N. Miura and Y. Takahashi. Int J Pres Ves Pip 2010; 87:58-65.